Determination of the $[Fe_4S_4]Cys_4$ cluster geometry of *Desulfovibrio africanus* ferredoxin I by ^1H NMR spectroscopy

Sharon L. Davy[a], Michael J. Osborne[a], Jacques Breton[a], Geoffrey R. Moore[a,*], Andrew J. Thomson[a], Ivano Bertini[b], Claudio Luchinat[c]

[a]*Centre for Metalloprotein Spectroscopy and Biology, School of Chemical Sciences, University of East Anglia, Norwich, NR4 7TJ, UK*
[b]*Department of Chemistry, University of Florence, Florence, Italy*
[c]*Institute of Agricultural Chemistry, University of Bologna, Bologna, Italy*

Received 2 February 1995; revised version received 15 March 1995

Abstract 1D and 2D ^1H NMR studies of the Fe_4S_4 cluster containing ferredoxin I from *Desulfovibrio africanus* have been carried out with the aim of determining the geometry of the cluster linkages with the 4 Cys side chains that bind the cluster. This required the Cys βCH resonances of the oxidised protein to be sequence-specifically and stereo-specifically assigned, and this was accomplished by a combination of TOCSY and NOE measurements, allied to model building based on X-ray structures of related ferredoxins. An analysis of the estimated hyperfine shifts of the Cys βCH resonances with a Karplus-type equation relating the shifts to iron-sulfur-β carbon-β proton dihedral angles, taken together with the relative relaxation rates of the two βCH_2 resonances, estimated from their linewidths, then allowed the iron-sulfur-β-carbon-α-carbon dihedral angles to be determined. A novel representation of the NMR data is presented which shows that the cluster dihedral angles are uniquely determined by the NMR data. The analysis reveals that the dihedral angles for *D. africanus* ferredoxin I are similar to the corresponding angles of other ferrredoxins even though there are differences in their ^1H NMR spectra. The sequence-specific and stereospecific assignments have been extended by analogy to the related Fe_4S_4-containing *D. gigas* ferredoxin I, and the stereospecific assignments to the Fe_4S_4-containing *Thermococcus litoralis* ferredoxin.

Key words: Ferredoxin; ^1H NMR; Structure; Iron-sulfur cluster; *D. africanus*

1. Introduction

Redox proteins containing Fe/S centres bound to cysteines, ferredoxins and HIPIPs, have been extensively studied, partly with the aims of determining their 3D structures, the electronic structures of their Fe/S clusters, and the relationships between these features and their cluster type and redox properties. Significant differences have been found between the environments of the ferredoxin and HIPIP clusters [1–3] but within the ferredoxin family there are marked similarities in structure which suggest that the ferredoxins share a common polypeptide folding pattern about the cluster, possibly because they are descended from a common ancestral protein [4]. Thus the X-ray structures of ferredoxins from *Bacillus thermoproteolyticus* (one Fe_4S_4 cluster) [5], *Peptococcus aerogenes* (two Fe_4S_4 clusters) [1] and *Azotobacter vinelandii* (one Fe_4S_4 cluster and one Fe_3S_4 cluster) [6], and the X-ray structure of ferredoxin II from *Desulfovibrio gigas* (one Fe_3S_4 cluster) [7] have many common features. However, the variation in their cluster types and redox properties is not understood at a structural level. With the development of NMR spectroscopy as a method for determining the 3D structures of diamagnetic proteins [8] and the electronic structures of paramagnetic centres [9], there has been considerable interest in comparative NMR studies of a range of ferredoxins to tackle these issues [10–17]. These studies have been given added impetus by the recent determination of the 3D structure of a HIPIP by NMR spectroscopy [18] and by the development of methods to assign NMR signals of cluster-ligating cysteines and to employ such data to define the electronic structure and geometry of the Fe/S cluster [19–21].

In the present paper, we report a 1D and 2D ^1H NMR study of the oxidized, Fe_4S_4 cluster-containing ferredoxin I from *D. africanus*. We show that by a combination of through-bond and through-space connectivity experiments, allied to molecular modelling based on known structures of other ferredoxins, a complete assignment of the cysteines ligating the cluster is attainable, and that these data, used in conjuncton with a recently described relationship linking the hyperfine shifts of the βCH_2 protons with the Fe-S-C_βH dihedral angles [21], allow the geometry and electronic structure of the cluster to be determined.

2. Materials and methods

D. africanus ferredoxin I was prepared for NMR as previously described[17]. All NMR experiments were carried out with the oxidised ferredoxin in 0.1 M phosphate, ^2H_2O, at pH* 6.2, where pH* refers to the direct pH meter reading and is uncorrected for any isotope effect. ^1H NMR spectra were recorded on Bruker AMX600 and JEOL GX-400 spectrometers. Chemical shift values were referenced to the residual H_2O peak at 4.75 ppm at 298 K. 2D-TOCSY spectra at 400 MHz were recorded by the procedure of [22] over a spectral width of 8,000–12,000 Hz. The spin-lock times were 5–25 ms and the size of the data sets was 1,024 × 256. For observation of NOESY effects at 600 MHz between fast relaxing species, mixing times of 5–10 ms were used as previously described [19]. 600 MHz 1D-NOE difference spectra were also collected as previously described [23]. Molecular modelling was carried out with QUANTA (Molecular Simulations, Cambridge, UK) running on an SG Indigo R4000 work station.

3. Results and discussion

3.1. Comparison of D. africanus and D. gigas ferredoxins I and B. thermoproteolyticus ferredoxin

The comparison of *B. thermoproteolyticus*. *D. gigas* and *D. africanus* ferredoxins is important for justifying the use of the *D. gigas* ferredoxin II and *B. thermoproteolyticus* X-ray structures in section 3.3.

*Corresponding author. Fax: (44) (1603) 259 396.
E-mail: G.MOORE@UEA.AC.UK

SSDI 0014-5793(95)00317-7

Fig. 1a shows the high-frequency region of the ^{1}H NMR spectrum of *D. africanus* oxidised ferredoxin I, and Table 1 reports the chemical shifts and linewidths of resonances a-j. Table 1 also contains comparable data for *D. gigas* ferredoxin I. The spectrum of *D. gigas* oxidised ferredoxin I has been reported, and the βCH_2 resonances of the cluster cysteines identified, by Macedo et al. [24] (see Table 1). Spectra of both ferredoxins contain well resolved peaks in the region 10 to 18 ppm that have temperature dependent chemical shifts and linewidths characteristic of resonances of cysteine cluster ligands. For example, in both cases the resolved resonances have increasing chemical shifts with increasing temperature, i.e. anti-curie behaviour. However, the pattern of chemical shifts is different from those of other Fe_4S_4 cluster containing ferredoxins [10–12] and thus assignment of the *D. africanus* and *D. gigas* ferredoxin I cysteine resonances cannot be made simply by comparison with characterised ferredoxins; additional NMR experiments, reported below, are required.

The spectra of oxidised *B. thermoproteolyticus* and *B. stearothermophilus* ferredoxins, which differ in one, amino acid residue only, have been reported by Nagayama et al. [25]. Resonance assignments were not obtained but the general appearance of the spectra in the region of 9–16 ppm is very similar to that of *D. africanus* ferredoxin I (Fig. 1a). In particular the two furthest high-frequency signals are at 15.6 and 13.8 ppm with an anti-curie temperature dependence. Thus, since the cysteine NMR characteristics are determined by the electronic properties of the cluster, it seems that *B. thermoproteolyticus* ferredoxin is a good model for the cluster of *D. africanus* ferredoxin I.

3.2. Identification of the cysteine ligand H_α and H_β resonances

The procedure we have employed to group the hyperfine shifted resonances into individual spin systems relies on the observation of TOCSY cross-peaks and NOE's between the geminal β-CH protons, and NOE's between the β-CH protons

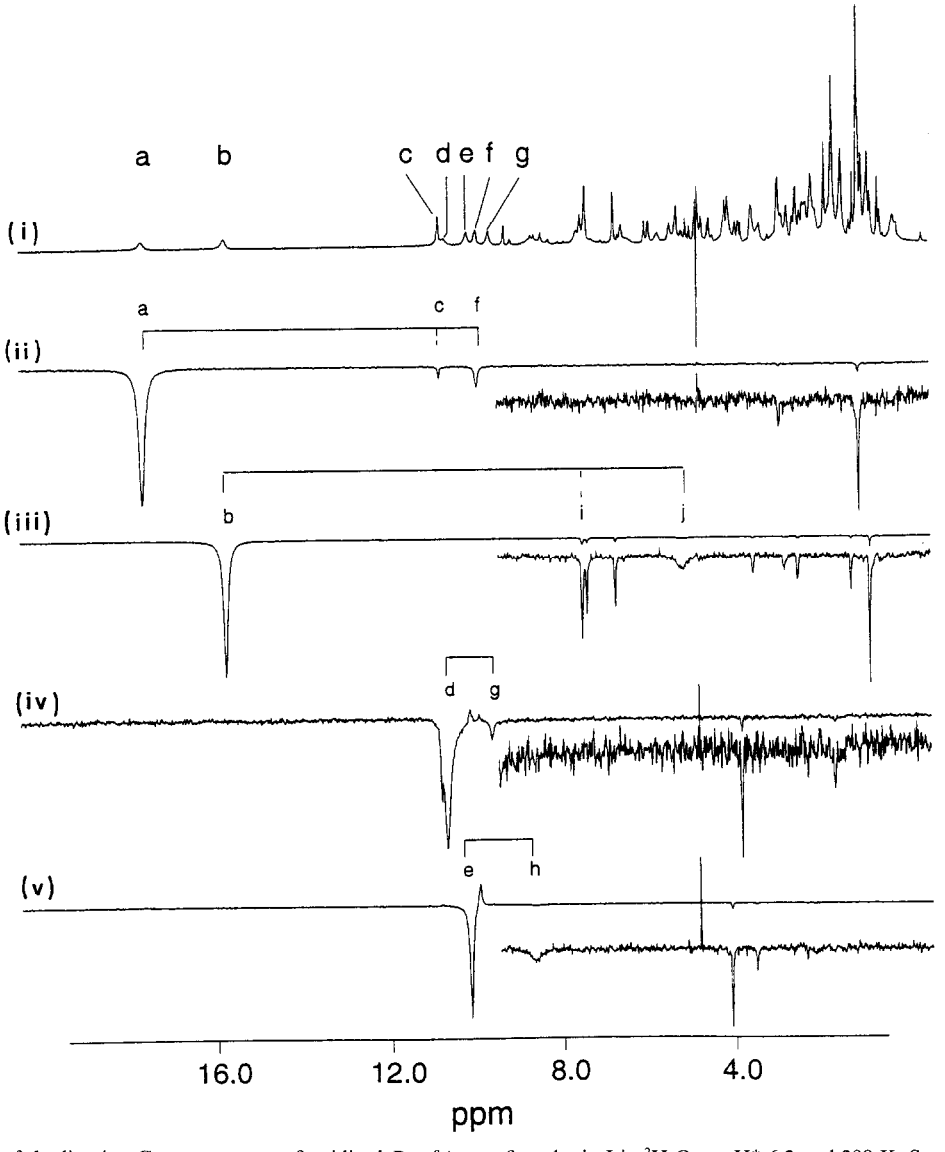

Fig. 1. Identification of the ligating Cys resonances of oxidised *D. africanus* ferredoxin I in ^2H_2O at pH* 6.2 and 298 K. Spectrum (i) is the normal spectrum and (ii), (iii), (iv) and (v) are the NOE difference spectra obtained on saturation of peaks a, b, d and e, respectively. From these difference spectra the pairwise assignment of the β-CH_2 resonances were obtained as follows: peaks a and f, peaks b and c, peaks d and g, and peaks e and h (see text).

and their corresponding α-CH proton. In general, it is expected that a β-CH to β-CH NOE will be stronger than a β-CH to α-CH NOE because the distance between the latter protons will be greater than the distance between the former protons. Also, in general, β-CH proton resonances should experience a larger paramagnetic shift than α-CH proton resonances. In some cases the α-CH resonances may be broader than the β-CH resonances, reflecting the relative distances of their protons from the iron.

A 400 MHz TOCSY spectrum of the oxidised ferredoxin in ^2H_2O with a mixing time of 11.5 ms contained cross-peaks linking the following pairs of resonances: a and f, b and j, d and g, and e and h (spectrum not shown). This identifies these four pairs of resonances as arising from the geminal βCH protons of the four cluster cysteines. This assignment is consistent with the NOE's reported in Fig. 1 which link together the pairs of resonances identified by the TOCSY experiment as cluster cysteine βCH resonances. This figure shows the 1D NOE difference spectra of *D. africanus* ferredoxin I obtained upon saturation of peaks a, b, d and e. From these data an assignment of the resonances to cysteines A, B, C and D is possible (Table 1). In addition the NOE difference spectra allow two αCH resonances to be assigned. For example, the strongest NOE on saturation of peak a is seen with peak f, indicating that these arise from geminal protons, and the second strongest NOE is with peak c, indicating that this is from the corresponding αCH proton.

The NOE difference spectra and the normal spectrum of *D. africanus* ferredoxin I in Fig. 1 show that different cysteine resonances have different linewidths. In all cysteines one of the βCH resonances is broader than its partner (Table 1). Line-broadening results from paramagnetic induced relaxation, and the closer the βCH proton is to an Fe of the cluster, the greater the line broadening. The observation of both a broad and a relatively sharp βCH resonance for each cysteine is consistent with previous NMR studies of ferredoxins, and with the various cluster geometries determined by X-ray crystallography: in all cases one βCH is closer to an Fe than the other βCH (Table 2). This is at variance with the HIPIP's, where Cys II has both βCH protons at about the same distance from the metal.

In summary, the NOE and TOCSY data account for all seven resonances downfield of 9.5 ppm, together with three peaks from the overlapped resonances between 5.0 and 8.6 ppm. Only ten of the twelve cysteine CH resonances have been clearly identified (Table 1). The remaining two αCH resonances may be too broad to be detected by the experiments carried out to date.

3.3. Sequence specific assignments of the cysteine ligand resonances

To obtain sequence specific assignments of the cysteine ligand resonances we have adopted the procedure used in comparable studies of HIPIP's and clostridial ferredoxins [21,26], namely using structures obtained from X-ray crystallography to predict what NOE's will be observed between particular cysteines and neighbouring amino acids that are not cluster ligands. During the course of our work the X-ray structure of *D. africanus* ferredoxin I was determined [27] but the coordinates are not yet available, and the X-ray structure of *D. gigas* ferredoxin I has not been reported. Therefore we have used the X-ray structure of the 82 amino acid, Fe_4S_4 cluster containing, ferredoxin from *B. thermoproteolyticus* [5], and the X-ray structure of the 58 amino acid, Fe_3S_4 cluster containing, ferredoxin II from *D. gigas* [7] as guides. Both structures were used because, though the *D. gigas* ferredoxin has a higher degree of sequence similarity to the *D. africanus* ferredoxin than does the *B. thermoproteolyticus* ferredoxin (see below), the latter ferredoxin contains the same type of Fe/S cluster to that of *D. africanus* ferredoxin I. *D. gigas* ferredoxin II has the same amino acid sequence as ferredoxin I from *D. gigas*, but the state of oligomerisation, as well as the cluster type, differs. Ferredoxin I is a monomer and ferredoxin II is a tetramer. Kissinger et al. [7], in their description of the X-ray structure of *D. gigas* ferredoxin II, remark that interconversion between the observed Fe_3S_4 cluster and an Fe_4S_4 cluster would probably only require a local adjustment of the polypeptide chain bearing the cysteine at the vacant iron site of the Fe_3S_4 cluster, as well as a significant readjustment of the cysteine side chain itself. Thus, the three coordinated cysteines should be little affected by the lack of a fourth iron; an observation consistent with the X-ray structure. Therefore we have confidence that the protein fold around the cluster can be used to help assignments for *D. africanus* ferredoxin I.

Using the sequence alignment given by Kissinger et al. [7],

Table 1
Sequence specific assignments and ^1H NMR spectral parameters of the Fe_4S_4 cluster ligating cysteine residues of *D. africanus* (this work)and *D. gigas* (ref. [24]) ferredoxins I

	D. africanus ferredoxin I*				*D. gigas* ferredoxin I**	
Signal	δ(ppm)	$\Delta\nu_{1/2}$(Hz)	Cysteine***	Sequence specific assignment	δ(ppm)	Cysteine assignment***
a	17.65	100	Aβ_2	Cys^{14}	16.9	$Cys^{11}\beta_2$
b	15.78	70	Bβ1	Cys^{17}	15.4	$Cys^{14}\beta_1$
c	10.82		Aα	Cys^{14}	11.3	$Cys^{8}\beta_1$
d	10.70	100	Cβ1	Cys^{11}	10.9	$Cys^{50}\beta_2$
e	10.15	50	Dβ2	Cys^{54}	10.7	$Cys^{11}\alpha$
f	9.95	45	Aβ1	Cys^{14}	10.2	$Cys^{11}\beta_1$
g	9.65	48	Cβ2	Cys^{11}	7.9	$Cys^{8}\beta_2$
h	8.63	150	Dβ1	Cys^{54}	7.4	$Cys^{14}\beta_2$
i	7.55		Bα	Cys^{17}	7.1	$Cys^{14}\alpha$
j	5.30	130	Bβ2	Cys^{17}	6.9	$Cys^{50}\beta_1$

* At pH* 6.2 and 298 K
** At pH* 7.6 and 293 K
***The justifications for the pairwise and stereospecific assignments of *D. africanus* ferredoxin I are given in the text. The assignments for the signals of *D. gigas* ferredoxin I [24] follow by analogy.

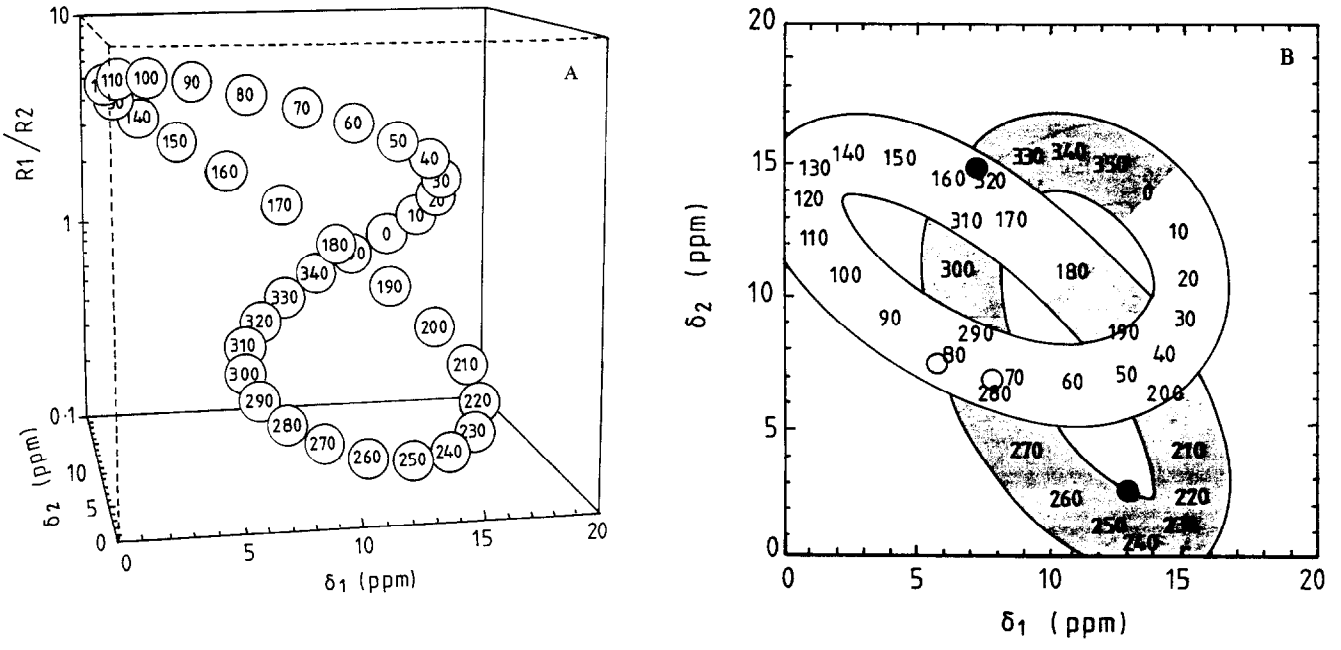

Fig. 2. Determination of the Fe-S-C_β-C_α dihedral angles from the estimated hyperfine shifts of the βCH_2 protons, δ_1 and δ_2, and their relative relaxation rates, R_1/R_2. (A) is a representation of the relationship between δ_1, δ_2 and R_1/R_2 for specified values of the Fe-S-C_β-C_α dihedral angle; and (B) is a projection of the 3D curve in (A) onto the δ_1/δ_2 plane. The projection in (B) is represented as a ribbon whose width represents the estimated error in assigning $\delta_c°$ to be entirely contact in origin, as well as the intrinsic errors in the coefficients of equation 1 [21]. The shaded part of the ribbon represents values of R_1/R_2 smaller than 1, and the open ribbon values of R_1/R_2 greater than 1. The δ_1, δ_2 and R_1/R_2 values for *D. africanus* ferredoxin I, calculated as described in the text, are indicated by open circles, for cysteines with R_1/R_2 greater than 1, and closed circles for cysteines with R_1/R_2 less than 1.

itself based on an alignment proposed by Bruschi and Guerlesquin [28], and correcting the sequence of *D. africanus* ferredoxin I as described by Davy et al. [17] and Séry et al. [27], gives an overall sequence identity between *D. africanus* ferredoxin I and the *D. gigas* and *B. thermoproteolyticus* ferredoxins of 39% and 25%, respectively. This rises to 55% and 41%, respectively, when the comparison is confined to the cluster binding regions of residues 5–26 and 50–56. The structural models for *D. africanus* ferredoxin I based on the X-ray structures of *D. gigas* ferredoxin II and *B. thermoproteolyticus* ferredoxin resemble each other well around the cluster, particularly in the important aspect of the amino acids that are near spatial neighbours of the cysteine ligands. It is this that allows the sequence specific assignments of the cysteine resonances to be made, as described below.

Saturation of peak b arising from Cys B produced NOE's to three peaks between 6 and 8 ppm (Fig. 1(iii)). Two of these have been assigned to Phe[25] by the sequential assignment procedure described by Wüthrich [8]. The model structures reveal that only Cys[17] is sufficiently close to Phe[25] for NOE's between them and thus Cys B is assigned to Cys[17]. The βCH_2 resonances of Phe[25], at 2.53 and 2.84 ppm, and resonances of Ala[50] at 3.54 and 0.89 ppm, also appear in the NOE difference spectrum and are consistent with the Cys[17] assignment. The remaining resonance in the NOE difference spectrum, at 7.52 ppm, comes from the Cys B αCH. Similarly, Cys D is assigned to Cys[54] because saturation of peak e produced a strong NOE to a resonance at 3.52 ppm (Fig. 1 (v)) that has been assigned to the α-CH proton of Met[51]. Both the *D. gigas* and *B. thermoproteolyticus* model structures show that only Cys[54] is sufficiently close to Met[51] to generate such an NOE. The peak at 4.08 ppm in the difference spectrum has not been unambiguously assigned and thus its appearance does not help identify Cys D as Cys[54].

The assignment of Cys A to Cys[14] and Cys C to Cys[11] given in Table 1 is less certain than the assignments of Cys[17] and Cys[54]. This is because peaks in the NOE difference spectra for these residues arising from other amino acids have not themselves been unambiguously assigned. Nevertheless, the tentative assignment of the cysteines is possible, as described below. The models show that for two cysteines, Cys[11] and Cys[54], their αCH protons are relatively close to the cluster, and closer than either of their β-CH protons (Table 2). Thus these are expected to be broad resonances, and therefore probably not detected in the NOE experiments. Certainly, the Cys[54] αCH resonance has not been detected. An αCH resonance is detected for Cys A but not for Cys C, and this is consistent with Cys A arising from Cys[14] leaving Cys C to come from Cys[11]. In support of this, the models indicate that the βCH protons of Cys[11] are close to more protons of other amino acids than are the βCH protons of Cys[14]. This means that there should be more NOE's from resonances of Cys[11] than from Cys[14]; and this is observed in Fig. 1 if the assignment of Cys A to Cys[14] (resonance a in Fig. 1 (ii)) and Cys C to Cys[11] (resonance d in Fig. 1 (iv)) is correct.

The stereo-specific assignments of the βCH protons in Table 1 comes from NOE measurements and from the relationship between linewidth (Table 1) and distance from an Fe (Table 2); the shorter the distance, the greater the linewidth. The proposed assignments are consistent with the structural models. For example, $H\beta_1$ of Cys[17] is closest to Phe[25] and it is irradiation of peak b that gives the strongest NOE to Phe[25] (Fig. 1 (iii)) rather than peak j (not shown). The analysis of hyperfine shifts in section 3.4 supports the stereospecific assignments in Table 1.

3.4. Determination of the Fe-S-C_β-C_α dihedral angles

The observed chemical shifts of the β-CH_2 protons of the coordinated cysteines reflect the amount of unpaired electron spin density transferred to them from the cluster Fe. Such transfer gives rise to a contact shift and it depends upon the dihedral angle θ formed by the Fe-S-C and S-C-H planes [21]. For $[Fe_4S_4]^{2+}$ cubane centres, the relationship betwen the observed contact shift ($\delta_c°$) and the angle θ has been shown to follow a Karplus type relationship [21] where

$$\delta_c = a\sin^2\theta + b\cos\theta + c \quad (1)$$

with $a = 11.5$, $b = -2.9$ and $c = 3.7$ ppm.

A virtually equivalent relationship was independently proposed from ENDOR data on a $[Fe_4S_4]^{3+}$ model compound [29]. $\delta_c°$ was obtained by subtraction of 2.8 ppm, the primary chemical shift of a Cys β-CH_2 proton resonance, from the observed chemical shift (Table 1). This analysis assumes that the entire difference between the intrinsic chemical shift and the observed chemical shift is contact in origin, and this is unlikely. Although a significant pseudo-contact contribution to the chemical shift is not expected, because there is negligible anisotropy of the magnetic susceptibility of the cluster [17], conformation dependent shifts arising from the proximity of aromatic residues or carbonyl groups to the Cys protons is possible. Nevertheless, the contact term will be the dominant one.

Use of equation [1] as such to obtain a unique θ value from $\delta_c°$ is prevented by its functional form, which yields more than one solution for most $\delta_c°$ values (up to 4 solutions, see Fig. 8 in ref.21). Considering the hyperfine shifts from both geminal βCH_2 protons (δ_1 and δ_2) reduces, but does not eliminate, the ambiguity. However, a qualitative use of relative relaxation rates for the βCH_2 protons (R_1/R_2) allows the ambiguity to be completely removed. This is illustrated in Fig. 2. Panel A shows a 3D representation of the relationship between δ_1, δ_2 and R_1/R_2. The δ_1/δ_2 relationship was obtained from equation **(1)** by substituting the appropriate values of angles for each proton ($\theta_1 = \theta - 120°$ and $\theta_2 = \theta + 120°$ where θ is the Fe-S-C_β-C_α dihedral angle), and R_1/R_2 was obtained as the ratio of the βCH_2 proton-Fe distances, $1/r_6$. The Fe-S-C_β-C_α dihedral angle was varied in steps of 10 degrees from 0 to 360, as can be seen in Fig. 2A. This diagram shows that the dihedral angle is uniquely defined by NMR data.

Fig. 2B shows the projection of the 3D curve in Fig. 2A onto the δ_1/δ_2 plane in a fashion similar to that already used for J-couplings in diamagnetic systems [30]. The δ_1, δ_2 and R_1/R_2 values for *D. africanus* ferredoxin I, calculated as described in the text from the shifts given in Table 1, and from the Fe–H distances given in Table 2, are plotted onto the projection in Fig. 2B. The Fe-S-C_β-C_α dihedral angles obtained from this are:

Cys^{11}: 75° Cys^{14}: 315° Cys^{17}: 245° and Cys^{54}: 80°

These angles, which are the first to be determined from NMR data, are similar to those of the refined X-ray structure of the two Fe_4S_4-cluster containing *P. aerogenes* ferredoxin [3]: cluster I 62°, 86°, 244° and 302°; cluster II 61°, 84°, 252° and 298°. Determination by NMR of environmental influences affecting the cluster geometry of *D. africanus* ferredoxin I, such as the number of hydrogen bonding interactions, awaits a full structure determination. This is in progress.

NMR data for the characterised ferredoxins from *C. pasteurianum* and *C. acidi urici* fall on the ribbon of Fig. 2 at the appropriate θ value, as expected since these data were employed to obtain equation **(1)** [21]. The corresponding data for *D. gigas* ferredoxin I, taken from Macedo et al. [24] and with the assignments given in Table 1, and the corresponding data for the Fe_4S_4 cluster containing ferredoxin from *Thermococcus litoralis* [31] also fit on the ribbon at similar θ values to those for *D. africanus* ferredoxin I. This similarity is perhaps not too surprising given the similarity in ferredoxin cluster geometries revealed by X-ray crystallography [1,3–7] but it shows that Fig. 2 is a powerful aid to resonance assignment provided θ values are known. Thus, for example, Donaire et al. [29] did not report the stereo-specific assignment of the Cys βCH_2 proton resonances of *T. litoralis* ferredoxin though they did have sufficient NMR data to obtain these provided the θ values are similar to those of other ferredoxins.

Table 2
Distances (Å) between the cluster Cys protons and the Fe atoms in the two hypothetical structural models based on X-ray coordinates of *D. gigas* (D.g) ferredoxin II [7] and *B. thermoproteolyticus* (B.t) ferredoxin [5]

		D.g	B.t
Cys^{11}	$H\beta_1$	3.39	3.51
	$H\beta_2$	4.33	4.36
	$H\alpha$	3.39	3.35
Cys^{14}	$H\beta_1$	–	4.30
	$H\beta_2$	–	3.50
	$H\alpha$	–	4.77
Cys^{17}	$H\beta_1$	4.19	3.94
	$H\beta_2$	3.19	2.82
	$H\alpha$	5.01	4.80
Cys^{54}	$H\beta_1$	3.10	3.36
	$H\beta_2$	4.16	4.34
	$H\alpha$	3.50	3.50

Acknowledgements: We thank the EPSRC for providing a Studentship to SLD, the Biomolecular Sciences Panel of the BBSRC and EPSRC for their support of the UEA Centre for Metalloprotein Spectroscopy and Biology, and the EC for their support of this work via their award of a Human Capital and Mobility (MASIMO) grant and their award of a 'large-scale facility' grant to the Florence laboratory. We also thank Professor C. Hatchikian (Marseille) for providing a sample of *D. africanus* ferredoxin I.

References

[1] Adman, E.T., Sieker, L.C. and Jensen, L.H. (1976) J. Biol. Chem. 251, 3801–3806.
[2] Carter Jr., C.W., Kraut, J., Freer, S.T and Alden, R.A. (1974) J. Biol. Chem. 249, 6339–6346.
[3] Backes, G., Mino, Y., Loehr, T.M., Meyer, T.E., Cusanovich, M.A., Sweeney, W.V., Adman, E.T. and Sanders-Loehr, J. (1991) J. Am. Chem. Soc. 113, 2055–2064.
[4] Fukuyama, K., Nagahara, Y., Tsukihara. T., Katsube, Y., Hase, T. and Matsubara, H. (1988) J. Mol. Biol. 199. 183–193.
[5] Fukuyama, K., Matsubara, H., Tsukihara. T. and Katsube, Y. (1989) J. Mol. Biol. 210, 383–398.
[6] Stout, C.D. (1989) J. Mol. Biol. 205, 545–555.
[7] Kissinger, C.R., Sieker, L.C., Adman, E.T. and Jensen, L.H. (1991) J. Mol. Biol. 219, 693–715.

[8] Wüthrich, K. (1986) NMR of Proteins and Nucleic Acids, Wiley, New York
[9] Bertini, I. and Luchinat, C. (1986) NMR of Paramagnetic Molecules in Biological Systems, Benjamin-Cummings, Menlo Park, California.
[10] Poe, M., Phillips, W.D., McDonald, C.C. and Lovenberg, W. (1970) Proc. Natl. Acad. Sci. USA 65, 797–804
[11] Bertini, I., Briganti, F., Luchinat, C., Messori, L., Monnanni, R., Scozzafava, A. and Vallini, G. (1992) Eur. J. Biochem. 204, 831–839
[12] Busse, S.C., La Mar, G.N. and Howard, J.B. (1991) J. Biol. Chem. 266, 23714–23723
[13] Macedo, A.L., Moura, I., Moura, J.J.G., Le Gall, J. and Huynh, B.H. (1993) Inorg. Chem. 32, 1101–1105
[14] Banci, L., Bertinin, I., Ciurli, S., Ferretti, S., Luchinat, C. and Piccioli, M. (1993) Biochemistry 32, 9387–9397
[15] Teng, Q., Zhou, Z.-H., Smith E.T., Busse, S.C., Howard, J.B., Adams, M.W.W. and La Mar, G.N. (1994) Biochemistry 33, 6316–6326.
[16] Chae, Y.-K., Abildgaard, F., Mooberry, E.S. and Markley, J.L. (1994) Biochemistry 33, 3287–3295.
[17] Davy, S.L., Breton, J., Osborne, M.J., Thomson, A.J., Thurgood, A.P., Lian, L-Y., Pétillot, Y., Hatchikian, C. and Moore, G.R. (1994) Biochim. Biophys. Acta 1209, 33–39
[18] Banci, L., Bertini, I., Eltis, L.D., Felli, I., Kastrau, D.H.W., Luchinat, C., Piccioli, M., Pierattelli, R. and Smith, M.K. (in press).
[19] Bertini, I., Briganti, F., Luchinat, C., Messori, L., Monnanni, R., Scozzafava, A. and Vallini, G. (1991) FEBS Lett. 289, 253–256.
[20] Sadek, M., Brownlee, R.T.C., Scrofani, S.D.B. and Wedd, A.G. (1993) J. Mag. Reson. B101, 309–314.
[21] Bertini, I., Capozzi, F., Luchinat, C., Piccioli, M. and Vila, A.J. (1994) J. Am. Chem. Soc. 116. 651–660.
[22] Bax, A. and Davis, D.G. (1985) J. Mag. Reson. 65, 355–360.
[23] Banci, L., Bertini, I. and Luchinat, C. (1994) Methods Enzymol. 239, 485–514.
[24] Macedo, A.L., Palma, P.N., Moura, I., LeGall, J., Wray, V. and Moura, J.J.G. (1993) Mag. Reson. Chem.
[25] Nagayama, K., Ozaki, Y., Kyogoku, Y., Hase, T. and Matsubara, H. (1983) J. Biochem. (Tokyo) 94, 893–902.
[26] Banci, L., Bertini, I., Ciurli, S., Ferretti, S., Luchinat, C. and Piccioli, M. (1993) Biochemistry 321, 9387–9397.
[27] Séry, A., Housset, D., Serre, L., Bonicel, J., Hatchikian, E.C., Frey, M. and Roth, M. (1994) Biochemistry (in press).
[28] Bruschi, M. and Guerlesquin, F. (1988) FEMS Microbiol. Rev. 54, 155–176.
[29] Monesca, J.M., Rius, G. and Lamotte, B. (1993) J. Am. Chem. Soc. 115, 4714–4731
[30] Tsikaris, V., Detsikas, E., Sakarellos-Daitsiotis, M., Sakarellos, C., Natzaki, E., Tzartos, S.J., Marraud, M. and Cung, M.T. (1993) Biopolymers 33, 1123–1134.
[31] Donaire, A., Gorst, C.M., Zhou, Z.H., Adams, M.W.W. and La Mar, G.N. (1994) J. Am. Chem. Soc. 116. 6841–6849.

Note added in proof

Since submission of the manuscript the X-ray structure of *D. africanus* ferredoxin I reported by Séry, A., Housset, D., Serre, L., Bonicel, J., Hatchikian, E.C., Frey, M. and Roth, M. [Biochemistry, in press] has become available through the Brookhaven Protein Data Bank [file: 1FXR]. The relevant Fe-S-C_β-C_α dihedral angles obtained from this structure are (with the NMR derived values reported in the present paper in parenthesis): Cys^{11}: 51.7° (75°); Cys^{14}: 316.0° (315°); Cys^{17}: 256.2° (245°); Cys^{54}: 75.4° (80°). With the exception of Cys^{11} there is excellent agreement between the NMR and X-ray determined values, and even with Cys^{11} there is reasonable agreement. A full structure determination by NMR, which is currently underway, is needed to investigate the source of the difference for Cys^{11}.